ANGELHY

Innovative solutions for design and strengthening of telecommunications and transmission lattice towers using large angles from high strength steel and hybrid techniques of angles with FRP strips

WORK PACKAGE 2 – DELIVERABLE 2.2

Proposal for design rules for single angle members

Coordinator:

National Technical University of Athens - NTUA, Greece

Beneficiaries:

ArcelorMittal Belval & Differdange SA - AMBD, Luxembourg

Universite de Liege - ULG, Belgium

COSMOTE Kinites Tilepikoinonies AE - COSMOTE, Greece

Centre Technique Industriel de la Construction Metallique - CTICM, France

SIKA France SAS - SIKA, France

Grant Agreement Number: 753993

AUTHORS:

UNIVERSITE DE LIEGE

Faculty of Applied Sciences, ArGEnCo Department

Quartier Polytech 1, Allée de la Découverte, 9, B52/3, 4000 Liège, Belgium

Authors: Marios-Zois Bezas, Jean-Pierre Jaspart, Jean-François Demonçeau

NATIONAL TECHNICAL UNIVERSITY OF ATHENS

Institute of Steel Structures

15780 Athens, Greece

Authors: Ioannis Vayas, Pavlos Thanopoulos, Dimitrios Vamvatsikos, Konstantinos Vlachakis, Maria-Eleni Dasiou

TABLE OF CONTENTS

1   Introduction

Angles exhibit special features compared with other common steel cross-sections in that they have only one axis of symmetry, their principal axes do not coincide with the geometrical axes and they are prone to torsional deformations due to their small rigidity in both uniform and non-uniform torsion. Consequently, design expressions for cross-section and member checks are expected to differ from those of other common shapes. However, EN 1993-1-1 [1] does not include any specific design rules for members composed of angle profiles when subjected to combined forces and moments.

Due to the absence of appropriate rules, design was performed by 2nd order analysis considering member bow imperfections, which was followed by cross-section checks with stress limitation to the yield or local buckling strength. Such an approach was proposed by the former German Code DIN 18800, part 2 [2]. In contrast, the US –Specifications included in a separate document [3] design rules for angles that took into account global, local and lateral torsional buckling and did not require 2nd order analysis at element level.

This report proposes rules for member design of equal angle sections subjected to combined forces and moments. The rules are of general use for the referred cross-sections. The application of the rules specifically to lattice towers and masts is presented in Deliverable 2.6. The rules were validated by numerical analyses and tests carried out during the current research project, as well as tests carried out in past investigations from the same and other authors.

2   Classification of angle profiles

2.1   Introduction and notation

According to EN 1993-1-1 [1], clause 5.5.2 (4) classification should be done for the compression parts of the cross-section that are defined as following: "Compression parts include every part of the cross-section which is either totally or partially in compression under the load combination considered". A strict application of this rule requires a separate classification of the cross-section for each combination of applied forces and moments. Since this rule is unpractical for design, a simpler approach is followed in practice, where the cross-section is classified separately for compression, strong axis bending and weak axis bending. This procedure is followed here, with one difference. For weak axis bending, the cross-section class may be different for positive or negative moments M_v due to the mono-symmetric shape of the profile that may lead to different classes when the tip is in compression o tension. Further on, the current document proposes a smooth transition between plastic and elastic bending resistances in a straightforward way.

The notation for the geometric, material and other properties follows the one given in EN 1993-1-1 [1].

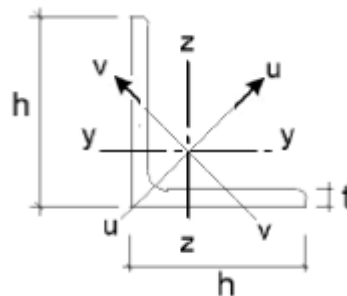**Figure 2.1: Notation for geometrical properties and principal axes**

2.2   Compression

2.2.1   General

According to EN 1993-1-1 [1], the section resistance to compression is determined from:

$$N_{c,Rd} = \frac{A \cdot f_y}{\gamma_{M0}} \qquad \text{for class 1, 2 or 3 cross-sections} \tag{2.1}$$

$$N_{c,Rd} = \frac{A_{eff} \cdot f_y}{\gamma_{M0}} \qquad \text{for class 4 cross-sections} \tag{2.2}$$

It may be seen that the resistance for sections to compression is identical for classes 1, 2 or 3. Accordingly, there is a need to define only the limit between classes 3 and 4.

It is noted that the failure modes for angle sections in compression may be distinguished in:

- Yielding of the cross section
- Local buckling of the legs
- Torsional buckling

Accordingly, the relevant failure mode for class 1 to 3 angle section is yielding, while for class 4 sections local buckling of the legs or torsional buckling. The limits for the two failure modes will be examined in the following.

2.2.2 Local buckling

The class 3 to class 4 limit may be determined by consideration of the **local buckling** resistance. The reduction factor of outstand plated elements due to local buckling is given by EN 1993-1-5 as below:

$$\rho = 1,0 \qquad \text{for} \qquad \bar{\lambda}_p \leq 0,748 \qquad (2.3)$$

$$\rho = \frac{\bar{\lambda}_p - 0,188}{\bar{\lambda}_p^2} \qquad \text{for} \qquad \bar{\lambda}_p > 0,748 \qquad (2.4)$$

where:

$$\bar{\lambda}_p = \sqrt{\frac{f_y}{\sigma_{cr}}} = \frac{\bar{b}/t}{28,4\varepsilon\sqrt{k_\sigma}} \qquad (2.5)$$

The condition for class 3 to class 4 limit is that the resistance to yielding should not be reduced due to local buckling. This may be written as:

$$\rho = 1 \qquad \text{or} \qquad \bar{\lambda}_p \leq 0,748 \qquad (2.6)$$

The buckling factor for outstand elements in compression (ψ=1) is according to EN 1993-1-5, Table 4.2, k_σ = 0,43. For equal leg angles EN 1993-1-5 defines $\bar{b}$ = h

Introducing the above in the expression for the limit slenderness, the class 3 to 4 limit in respect tolocal buckling may be calculated:

$$\rightarrow \quad h/t \leq 13,9\varepsilon \qquad (2.7)$$

2.2.3 Torsional buckling

Condition (2.7) is expressing the susceptibility of the angle legs to local buckling considering them as outstand elements simply supported at the root. The hinged support at the edge of the outstand element presumes an independent buckling of the two legs. However for compression load, the question is if local buckling of one leg does adversely influence the other. This may be studied by

examination of the resistance to **torsional buckling.** In this failure mode the cross section rotates along its shear center, i.e. along the angle heel.

The critical load for this buckling mode may be determined for an angle section regarded as a two plate setion, Fig.2.1.
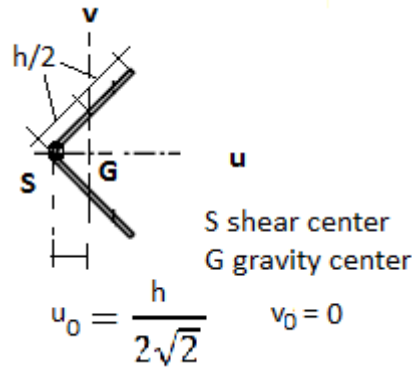

Figure 2.2: Notation for the idealized section

The properties of this section are as following:

Cross-section area: $\qquad A = 2\,h\,t$ (2.8)

Second moment of area: $\quad I_u = \dfrac{A \cdot h^2}{6}$ (2.9) $\qquad\qquad\qquad I_v = \dfrac{A \cdot h^2}{24}$ (2.10)

Warping constant: $\qquad\qquad I_w = \dfrac{1}{1-\mu^2} \cdot \dfrac{h^3 \cdot t^3}{18} \sim 0$ (2.11)

Torsion constant $\qquad\qquad I_t = \dfrac{2 \cdot h' \cdot t^3}{3}$ (2.12)

The critical buckling load for torsional buckling may be determined from:

$$N_{cr,T} = \frac{1}{i_0^2}\left(GI_t + \frac{\pi^2 E I_w}{l_T^2}\right)$$ (2.13)

where:

$$i_0^2 = i_u^2 + i_v^2 + u_0^2 + v_0^2$$ (2.14)

u_0 , v_0 see Fig. 2.1

or $\quad i_0^2 = \dfrac{h^2}{6} + \dfrac{h^2}{24} + \dfrac{h^2}{8} + 0 = \dfrac{h^2}{3}$ (2.15)

Introducing the above properties, the critical torsional buckling load may be written as:

$$N_{cr,T} = \frac{G \cdot 2ht^3/3}{h^2/3} = 2G\frac{t^3}{h}$$ (2.16)

And the critical torsional buckling stress as:

$$\sigma_{cr,T} = G \frac{t^2}{h^2} \tag{2.17}$$

The relative slenderness to torsional buckling is written as:

$$\bar{\lambda}_T = \sqrt{\frac{f_y}{\sigma_{cr,T}}} = \frac{h/t}{18,5\varepsilon} \tag{2.18}$$

The condition for torsional buckling not influencing local buckling may be written as:

$$\sigma_{cr,T} \geq f_y \qquad (2.19) \qquad \rightarrow \qquad \bar{\lambda}_T \leq 1 \ (2.20) \qquad \rightarrow$$

$$h/t \leq 18,5\varepsilon \tag{2.21}$$

It may be seen that the limit h/t-ratio for local buckling supersedes the corresponding ratio for torsional buckling.

2.2.4 Eurocode 3 provisions and conclusion

The class-3 limit for angle sections to compression is provided by EN 1993-1-1, Table 5.2, sheet 3 as below. Both conditions listed in the Table shall be fulfilled. Accordingly, for equal leg angles with h=b the class-3 limit is given by:

$$h/t \leq 11,5\varepsilon \tag{2.22}$$

In addition, EN 1993-1-1, Table 5.2, sheet 3 makes cross reference to sheet 2 "outstand elements", as indicated with red above. It is unclear how to understand this reference, since sheet 2 refers to "compression parts" which might be applicable also for angles in bending. An answer could be given by comparison of the provisions of the two sheets. Indeed, according to sheet 2 the class-3 limit is given by:

$$c/t \leq 14\varepsilon \tag{2.23}$$

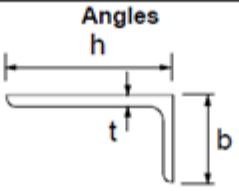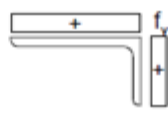**Table 2.1: Class-3 limit for angles in compression to EN 1993-1-1 (EN 1993-1-1, Table 5.2, sheet 3)**

Table 2.2: Classification for outstand elements to EN 1993-1-1 (EN 1993-1-1, Table 5.2, sheet 2)

Class	Part subject to compression	Part subject to bending and compression	
		Tip in compression	Tip in tension
Stress distribution in parts (compression positive)			
1	$c/t \leq 9\varepsilon$	$c/t \leq \dfrac{9\varepsilon}{\alpha}$	$c/t \leq \dfrac{9\varepsilon}{\alpha\sqrt{\alpha}}$
2	$c/t \leq 10\varepsilon$	$c/t \leq \dfrac{10\varepsilon}{\alpha}$	$c/t \leq \dfrac{10\varepsilon}{\alpha\sqrt{\alpha}}$
Stress distribution in parts (compression positive)			
3	$c/t \leq 14\varepsilon$	$c/t \leq 21\varepsilon\sqrt{k_\sigma}$ For k_σ see EN 1993-1-5	

$\varepsilon = \sqrt{235/f_y}$	f_y	235	275	355	420	460
	ε	1,00	0,92	0,81	0,75	0,71

The comparison between (2.22) and (2.23) indicates that c/h = 14/11,5 >1 which is not true because it is always c < h, i.e. c/h < 1.

The above considerations and analytical derivations lead to the final conclusion that the class-3 limit for angles subjected to compression may be set as following:

h/t ≤ 14ε   (2.24)

This condition:

- is in line with current provisions of Eurocode 3 and more specifically EN 1993-1-1sheet 2 for class-3 limit of outstand elements
- covers local buckling and torsional buckling

2.3 Bending

2.3.1 General

The bending resistance of cross-sections in respect to the principal axes may be determined according to EN 1993-1-1, 6.2.5 as following:

$$M_{c,Rd} = M_{pl,Rd} = \frac{W_{pl} \cdot f_y}{\gamma_{M0}} \quad \text{for class 1 or 2 cross-sections} \tag{2.25}$$

$$M_{c,Rd} = M_{el,Rd} = \frac{W_{el,min} \cdot f_y}{\gamma_{M0}} \text{ for class 3 cross-sections} \tag{2.26}$$

$$M_{c,Rd} = \frac{W_{eff,min} \cdot f_y}{\gamma_{M0}} \qquad \text{for class 4 cross-sections} \tag{2.27}$$

It may be seen that the design resistance for classes 1 and 2 is identical, the plastic one. The two classes differ in the possibility to apply plastic methods of analysis for class 1 sections, while for class 2 sections elastic methods shall be employed. However, plastic methods of analysis are rarely used in towers composed of angle sections. Therefore, the two classes 1 and 2 are merged in the following and only limits between classes 2 and 3 and 3 and 4 will be derived. In addition, those limits will be given separately for bending on the strong and the weak axis.

The limit width-to-thickness values between classes for outstand elements are provided by EN 1993-1-1, Table 5.2, sheet 2, see Table 2 above. The above limits could be used for angle sections whose legs are outstand elements. In the following rules will be derived for angle sections that allow a straightforward and simpler classification in classes for principal axis bending.

2.3.2 Strong axis bending M_u

The stress distribution for strong axis bending is shown in Fig. 2.2. It may be seen that only one leg is under compression and needs classification.
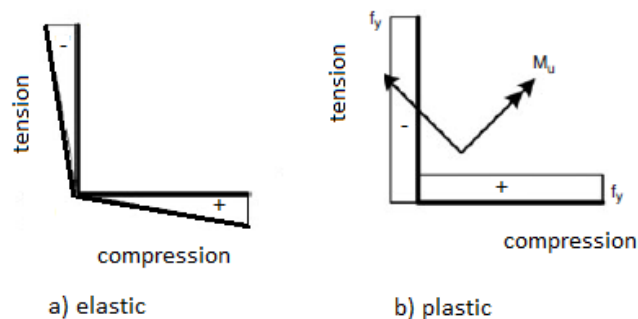

Figure 2.3: Stress distribution for strong axis bending (M_u)

Table 2.3: Buckling factors for outstand elements to EN 1993-1-1 (EN 1993-1-1, Table 4.2)

Stress distribution (compression positive)				Effective[p] width b_{eff}
				$1 > \psi \geq 0$: $b_{eff} = \rho \, c$
				$\psi < 0$: $b_{eff} = \rho \, b_c = \rho \, c \, / \, (1-\psi)$
$\psi = \sigma_2/\sigma_1$	1	0	-1	$1 \geq \psi \geq -3$
Buckling factor k_σ	0,43	0,57	0,85	$0,57 - 0,21\psi + 0,07\psi^2$

For elastic behavior the compression leg is an outstand element subjected to a stress ration $\psi = 0$, when considering the overall width of the leg, h. The corresponding buckling factor $k_\sigma = 0{,}57$ (see Table 3 above). The class 3 limit may be obtained from the general formula of EN 1993-1-1, Table 5.2, sheet 2, see Table 2 from:

$$\frac{h}{t} \le 21\varepsilon\sqrt{0{,}57} = 16\varepsilon \tag{2.28}$$

Setting $c \approx 0{,}85$ h, the above condition provides the limit for elastic behavior, i.e. the limit between classes 3 and 4.

$$\frac{c}{t} \le 14\varepsilon \tag{2.29}$$

For plastic behavior the leg is an outstand element subjected to uniform compression Class 2 limit may be obtained from EN 1993-1-1, Table 5.2, sheet 2, see Table 2:

$$\frac{c}{t} \le 10\varepsilon \tag{2.30}$$

or alternatively setting $c \approx 0{,}8$ h

$$\frac{h}{t} \le 12\varepsilon \tag{2.31}$$

That defines the limit between classes 2 and 3.

2.3.3 Weak axis bending M_v

When the cross-section is subjected to weak axis bending, the stress conditions for the two legs are identical. Accordingly, classification refers to both legs.

The stress distribution for **tip in tension** is shown in Fig. 2.3. The stress ratio for elastic stress distribution is given by $= \frac{\sigma_2}{\sigma_1} = -\frac{h-e}{e-(h-c)}$. For usual angle sections it is $\psi < -1$, so that the buckling factor is larger than $k_\sigma = 23{,}8$ (EN 1993-1-5, Table 4.2). The class 3 limit may be accordingly obtained from the general formula of EN 1993-1-1, Table 5.2, sheet 2, see Table 2 from:

$$\frac{c}{t} \le 21\varepsilon\sqrt{23{,}8} = 102\varepsilon \approx 100\varepsilon \tag{2.32}$$

It may be seen that, practically, all angle sections are at least class 3 for the case under consideration (weak axis bending tip in tension).

For the plastic stress distribution, the proportion of the leg to compression is:

$$\alpha = \frac{e_p - t - r}{h - t - r} \tag{2.33}$$

and taking as an approximation r = t, it may be shown that for usual angle sections it is $\alpha = 0{,}4$, Fig. 2.4. The class 2 limit may be accordingly obtained from the general formula of EN 1993-1-1, Table 5.2, sheet 2, see Table 2 from:

$$\frac{c}{t} \le \frac{10\varepsilon}{a\sqrt{a}} = \frac{10\varepsilon}{0{,}4\sqrt{0{,}4}} = 40\varepsilon \tag{2.34}$$

Accordingly, all angle sections may practically always develop their plastic moment for weak axis bending when the tip is in tension.

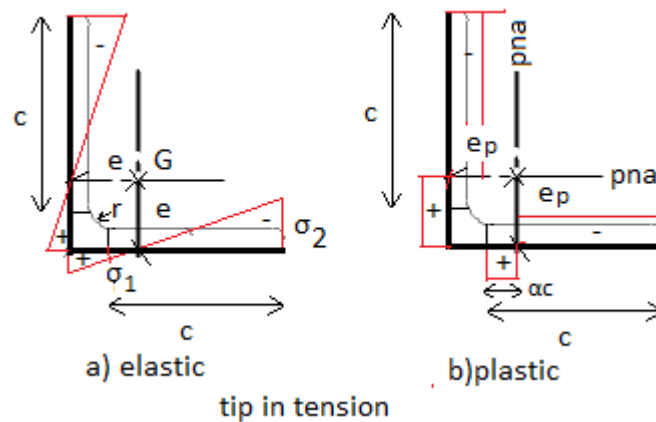

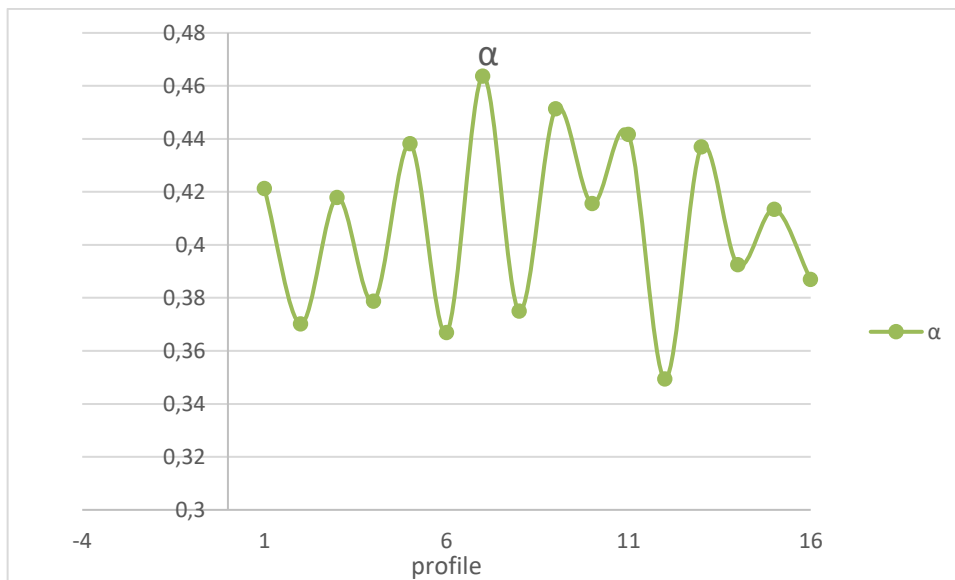**Figure 2.4: Stress distribution for weak axis bending (M_v) – tip in tension**

Figure 2.5: Ratios α for tip in tension (angles from 70 to 300)

The stress distribution for **tip in compression** is shown in Fig. 2.5. The stress ratio for elastic stress distribution is given by $\psi = \frac{\sigma_2}{\sigma_1} = -\frac{e-(h-c)}{h-e}$ which is the reverse of ψ for tip in tension. Fig. 2.6 shows that it is ψ ≈ -0,1 for usual angle sections, so that on the safe side the buckling factor may be set equal to $k_\sigma = 0,57$, valid for ψ = 0 (Table 3 above). The class 3 limit may be accordingly obtained from the general formula of EN 1993-1-1, Table 5.2, sheet 2, see Table 2, from the condition:

$$\frac{c}{t} \leq 21\varepsilon\sqrt{0,59} = 16\varepsilon \tag{2.35}$$

For the plastic stress distribution, it is α = 1 - 0,4 = 0,6. The class 2 limit may be accordingly obtained from the general formula of EN 1993-1-1, Table 5.2, sheet 3, see Table 2, from:

$$\frac{c}{t} \leq \frac{10\varepsilon}{a} = \frac{10\varepsilon}{0,4} = 16,6\varepsilon \tag{2.36}$$

Equations (2.35) and (2.36) are in contradiction due to the fact that the former obtains a smaller c/t-ratio for class 3 compared to class 2 that is given by the latter. The reason is that the mechanical model for class 2 sections of Eurocode 3 when the tip is in compression is not correct. Indeed, as shown in Fig. 8, outstand elements partially in compression are treated as elements full in compression with a reduced width αc. This means that the hinge support is introduced exactly at the position where the compression starts. This is questionable, since tension is beneficial to local buckling, but possibly not as much as to provide a full support. For that reason, it is proposed here to keep the c/t limit for class 3 and reduce it for class 2 to $\frac{c}{t} \leq 14\varepsilon$.

a) elastic   b) plastic
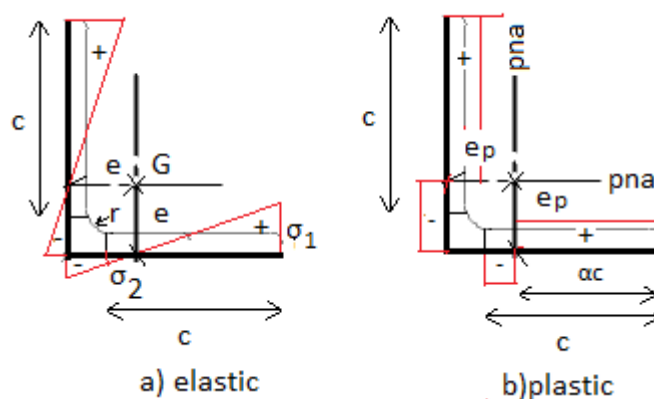
Figure 2.6: Stress distribution for weak axis bending (M_v) – tip in compression
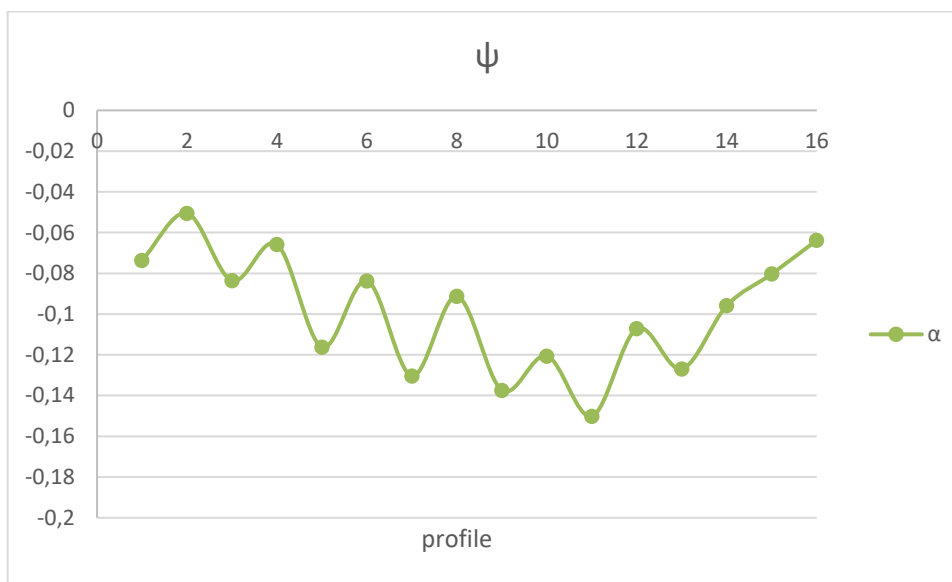

Figure 2.7: Stress ratio ψ for elastic stress distribution – tip in compression (angles from 70 to 300)
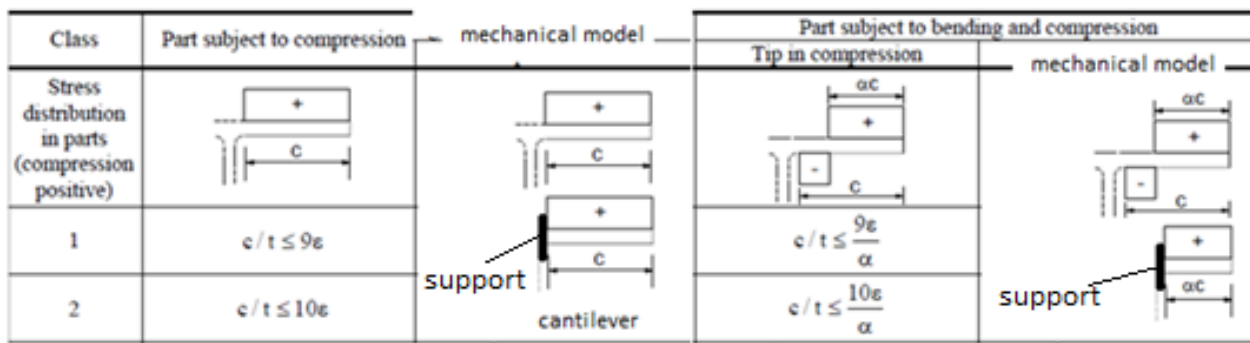
Figure 2.8: Mechanical model for outstand elements – tip in compression

2.3.4   Conclusion

The results of the above analyses conclude with Table 2.4 that presents the proposed classification limits for angle cross-sections.

Table 2.4: Proposal for classification of equal leg angle cross-sections

	Comment	Class 3	Class 2
Compression N_c		$\dfrac{h}{t} \leq 14\varepsilon$	
Strong axis bending M_u		$\dfrac{c}{t} \leq 14\varepsilon$	$\dfrac{c}{t} \leq 10\varepsilon$
Weak axis bending M_v	**Tip in tension**	$\dfrac{c}{t}$ any	
	Tip in compression	$\dfrac{c}{t} \leq 16\varepsilon$	$\dfrac{c}{t} \leq 14\varepsilon$

3 Member design

3.1 Tension

The design resistance of angle cross-sections to tension is given by:

- Gross section: $N_{t,Rd} = \dfrac{Af_y}{\gamma_{M0}}$ (3.1)

- Net section: $N_{t,Rd} = \dfrac{0,9A_{net}f_u}{\gamma_{M2}}$ (3.2)

- For angles connected $N_{t,Rd}$

3.1.1 Compression Class 1, 2 and 3 cross-sections

Strong axis buckling: $N_{bu,Rd} = \dfrac{\chi_u Af_y}{\gamma_{M1}}$ (3.3)

Weak axis buckling: $N_{bv,Rd} = \dfrac{\chi_v Af_y}{\gamma_{M1}}$ (3.4)

Design resistance: $N_{b,Rd} = \min\{N_{bu,Rd}, N_{bv,Rd}\}$ (3.5)

Relative slenderness strong axis: $\bar{\lambda}_u = \sqrt{\dfrac{Af_y}{N_{cr,u}}}$ (3.6)

Relative slenderness weak axis: $\bar{\lambda}_v = \sqrt{\dfrac{Af_y}{N_{cr,v}}}$ (3.7)

Reduction factors χ_u, χ_v as functions of the slenderness derived from buckling curve **b**

$\chi_{min} = \min\{\chi_u, \chi_v\}$ (3.8)

3.1.2 Class 4 cross-sections

Strong axis buckling: $N_{bu,Rd} = \dfrac{\chi_u A_{eff}f_y}{\gamma_{M1}}$ (3.9)

Weak axis buckling: $N_{bv,Rd} = \dfrac{\chi_v A_{eff}f_y}{\gamma_{M1}}$ (3.10)

Design resistance: $N_{b,Rd} = \min\{N_{bu,Rd}, N_{bv,Rd}\}$ (3.11)

Reduction factors χ_u, χ_v as for class 1 to 3 cross-sections

$\chi_{min} = \min\{\chi_u, \chi_v\}$ (3.12)

Area of effective cross-section: $A_{eff} = \rho \cdot A$ (3.13)

where:

Relative plate slenderness of legs: $\bar{\lambda}_p = \sqrt{\dfrac{\sigma_{com}}{\sigma_{cr}}} = \sqrt{\dfrac{\sigma_{com}}{f_y}}\sqrt{\dfrac{f_y}{235}}\sqrt{\dfrac{235}{\sigma_{cr}}} = \sqrt{\chi_{min}}\dfrac{h/t}{18,6\varepsilon}$ (3.14)

Reduction factor for plate buckling:

- $\rho = 1$ for $\bar{\lambda}_p \leq 0,751$ (3.15)

- $\rho = \dfrac{\bar{\lambda}_p - 0,188}{\bar{\lambda}_p^2}$ for $\bar{\lambda}_p > 0,751$ (3.16)

3.1.3 Justification

The buckling resistance of class 1, 2 and 3 cross-sections follows EN 1993-1-1 [1], eq. (6.47). The selection of buckling curve b follows the provisions of EN 1993-1-1 [1], Table 6.2 for L-sections. This is to be verified numerically-experimentally.

For the buckling resistance of class 4 cross-sections EN 1993-1-1 [1], eq. (6.48) is used. However, the interaction between local and global buckling are considered in the definition of the relative plate slenderness $\bar{\lambda}_p$ and not the global member slenderness $\bar{\lambda}$, unlike in EN 1993-1-1 [1], 6.3.1.2 (1). This is to be verified numerically-experimentally.

3.2 Strong axis bending
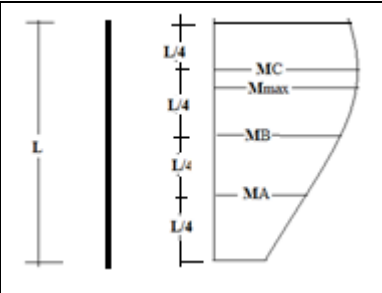
The design resistance of angle cross-sections to strong axis bending considering the effects of lateral torsional buckling (LTB) is given by:

$$M_{u,Rd} = \chi_{LT} W_u \frac{f_y}{\gamma_{M1}} \tag{3.17}$$

3.2.1 Determination of $\bar{\lambda}_{LT}$ and χ_{LT}

Critical LTB moment: $M_{cr} = C_b \dfrac{0{,}46 \cdot E \cdot h^2 \cdot t^2}{l}$ (3.18)

Table 3.1: Determination of the C_b-factor for LTB

$$C_b = \frac{12.5 M_{\max}}{2.5 M_{\max} + 3 M_A + 4 M_B + 3 M_C} \leq 1.5$$

For linear moment distribution with $-1 \leq \psi = \dfrac{M_2}{M_1} \leq 1$

$C_b = \dfrac{12{,}5}{7{,}5 + 5\psi}$

Slenderness to LTB $\bar{\lambda}_{LT} = \sqrt{\dfrac{W_u \cdot f_y}{M_{cr}}}$ (3.19)

Reduction factor χ_{LT} as function of the LTB slenderness derived from buckling curve **d**

Note: LTB may be ignored and χ_{LT} set to $\chi_{LT} = 1$ when one of the following conditions apply:

- $\bar{\lambda}_{LT} \leq \bar{\lambda}_{LT,0}$ with $\bar{\lambda}_{LT,0} = 0{,}4$
- $\dfrac{M_{Ed}}{M_{cr}} \leq \bar{\lambda}_{LT,0}^{2}$
- $\dfrac{N_{Ed}}{N_{bu,Rd}} > 0{,}5$
- $\dfrac{N_{Ed}}{N_{bv,Rd}} > 0{,}5$

3.2.2 Determination of W_u

$$W_u = \alpha_{i,u} W_{el,u} \quad \text{i = 2 or 3 or 4} \tag{3.20}$$

➢ Parameter $\alpha_{i,u}$

- Class 1 or 2: $\alpha_{2,u} = 1,5$ (3.21)

- Class 3   : $\alpha_{3,u} = \left[1 + \left(\frac{14\varepsilon - c/t}{14\varepsilon - 10\varepsilon}\right) \cdot (1,5 - 1)\right]$ (3.22)

- Class 4   : $\alpha_{4,u} = W_{eff,u} / W_{el,u} = 1,30 \, \rho_u$ (3.23)

relative plate slenderness of legs: $\bar{\lambda}_p = \sqrt{\frac{\sigma_{com}}{\sigma_{cr}}} = \sqrt{\frac{\sigma_{com}}{f_y}} \sqrt{\frac{f_y}{235}} \sqrt{\frac{235}{\sigma_{cr}}} = \sqrt{\chi_{LT}} \frac{c/t}{18,6\varepsilon}$ (3.24)

Reduction factor for plate buckling:

- $\rho_u = 1$ for $\bar{\lambda}_p \le 0,751$ (3.25)

- $\rho_u = \frac{\bar{\lambda}_p - 0,188}{\bar{\lambda}_p{}^2}$ for $\bar{\lambda}_p > 0,751$ (3.26)

3.2.3 Justification

The LTB-resistance is in line with EN 1993-1-1 [1], eq. (6.55). However, as in flexural buckling, the interaction between local and global buckling are considered in the relative plate slenderness $\bar{\lambda}_p$ and not in the global slenderness $\bar{\lambda}_{LT}$. This is to be verified numerically-experimentally.

The critical LTB-moment is derived from the literature, the C_b– value from the LRFD-Code [4].

Buckling curve d is adopted following the *General case* of Eurocode, EN 1993-1-1 [1], 6.3.2.2. This is to be verified numerically-experimentally.

The transition between elastic and plastic bending resistances adopts the results of SEMICOMP. Since they were derived for I-cross-sections, their validity should be checked numerically-experimentally for angle sections.

For strong axis bending, the effective cross-section becomes non-symmetric due to the fact that only one leg is in compression. This changes the position of the centroid, the directions of the principal axes and all cross-section properties. In order to avoid such laborious calculation an approximate solution for the effective section modulus is envisaged. This may be achieved by reducing equally the other leg too as in Fig. 3.1. The comparison of the ratio between the two cross-sections is shown in Fig. 3.2. It may be seen that the modulus of the effective cross-section it larger that the modulus of the initial cross-section multiplied with the reduction factor ρ by a factor ranging from 1.27 to 1.38 (for the cross-sections considered). Accordingly, a value 1,30 was adopted.
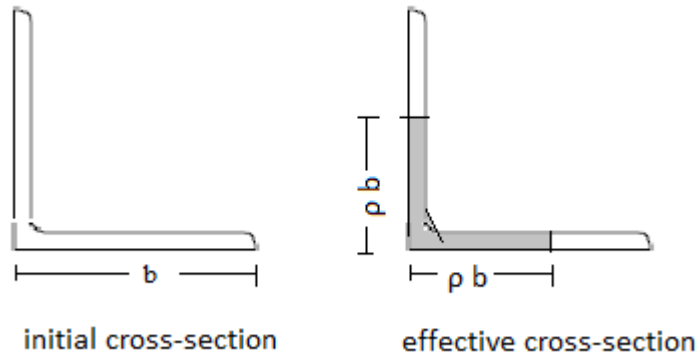
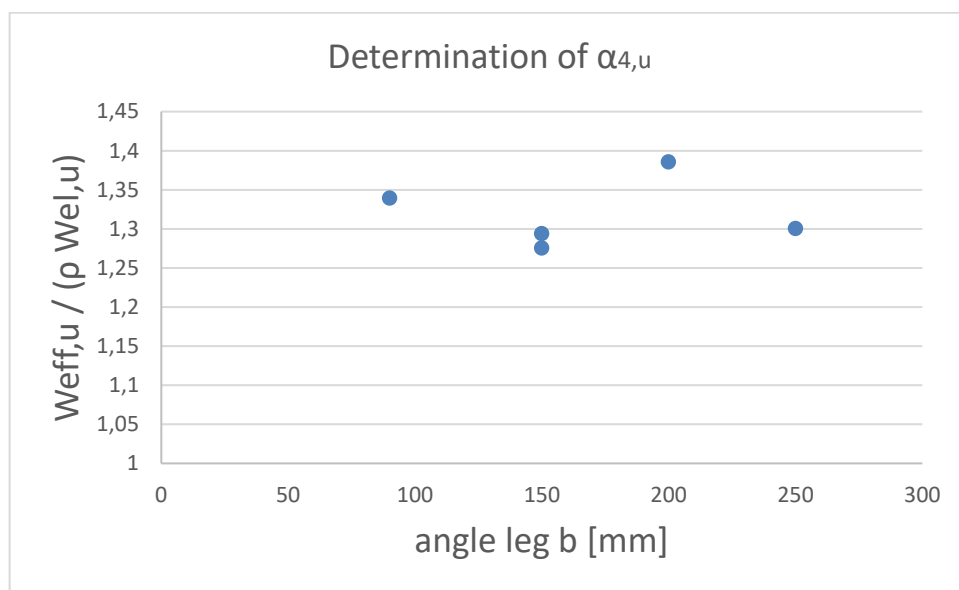**Figure 3.1: Initial and effective cross-section**

Figure 3.2: Ratio of the strong axis moduli between the initial and the effective cross-section

3.3   Weak axis bending

The design resistance of angle cross-sections to weak axis bending is given by:

$$M_{v,Rd} = W_v \frac{f_y}{\gamma_{M1}} \tag{3.27}$$

3.3.1 Determination of W_v

> ➢ Tip in tension

$W_v = 1{,}5\, W_{el,v}$ (3.28)

> ➢ Tip in compression

$W_v = \alpha_i W_{el,v} \quad i = 2 \text{ or } 3 \text{ or } 4$ (3.29)

▪ Class 1 or 2 section: $\alpha_2 = 1{,}5$ (3.30)

- • Class 3   section: $\alpha_3 = \left[1 + \left(\frac{16\varepsilon - c/t}{16\varepsilon - 14\varepsilon}\right) \cdot (1,5 - 1)\right]$ (3.31)

- • Class 4   section: $\alpha_4 = W_{\text{eff,v}} / W_{\text{el,v}} = \rho_v^2$ (3.32)

relative plate slenderness of legs: $\bar{\lambda}_p = \sqrt{\frac{f_y}{\sigma_{\text{cr}}}} = \sqrt{\frac{f_y}{235}} \sqrt{\frac{235}{\sigma_{\text{cr}}}} = \frac{c/t}{21,3\varepsilon}$ (3.33)

Reduction factor for plate buckling:

- • $\rho_v = 1$ for $\bar{\lambda}_p \leq 0,751$ (3.34)

- • $\rho_v = \frac{\bar{\lambda}_p - 0,188}{\bar{\lambda}_p^2}$ for $\bar{\lambda}_p > 0,751$ (3.35)

3.3.2 Justification

For tip in tension or class 1 or 2 sections, the plastic resistance with the shape factor 1,5 is employed. The transition between elastic and plastic bending resistances adopts the results of SEMICOMP. They are subject to numerical-experimental verification for angle sections.

For class 4 cross-sections a similar procedure as for strong axis bending is adopted. Fig. 3.3 shows that the modulus of the effective cross section is approximately equal to the modulus of the initial cross-section multiplied with the square of the reduction factor, ρ^2. α_4 is therefore fixed accordingly.
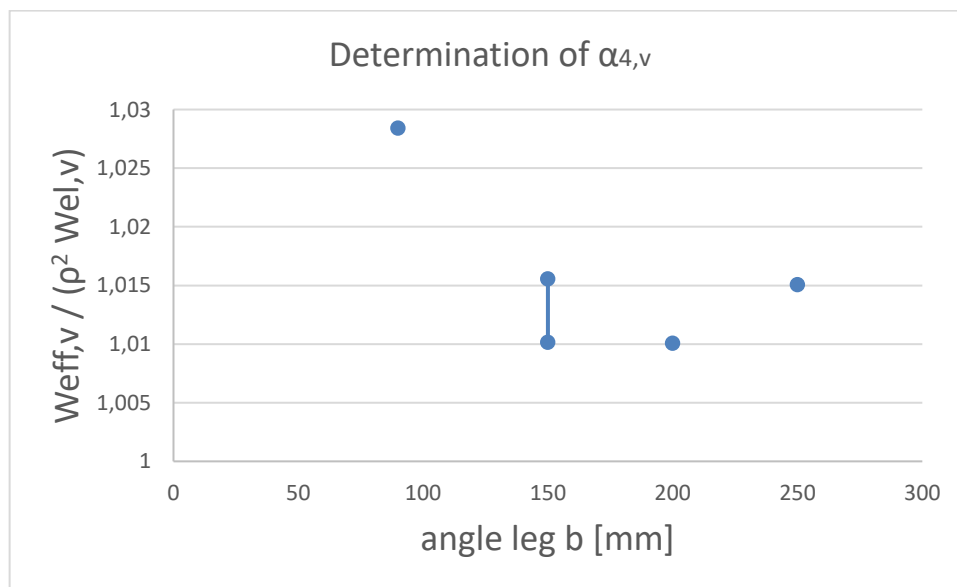
Figure 3.3: Ratio of the weak axis moduli between the initial and the effective cross-section

3.4 Resistance to combined compression and bending

3.4.1 Strong axis check

$$\left(\frac{N_{Ed}}{N_{bu,Rd}} + k_{uu}\frac{M_{u,Ed}}{M_{u,Rd}}\right)^{\xi} + k_{uv}\frac{M_{v,Ed}}{M_{v,Rd}} \leq 1$$ (3.36)

3.4.2 Weak axis check

$$\left(\frac{N_{Ed}}{N_{bv,Rd}} + k_{vu}\frac{M_{u,Ed}}{M_{u,Rd}}\right)^{\xi} + k_{vv}\frac{M_{v,Ed}}{M_{v,Rd}} \leq 1 \tag{3.37}$$

3.4.3 Factors

$$k_{uu} = \frac{C_u}{1-\frac{N_{Ed}}{N_{cr,u}}} \tag{3.38}$$

$$k_{uv} = C_v \tag{3.39}$$

$$k_{vu} = C_u \tag{3.40}$$

$$k_{vv} = \frac{C_v}{1-\frac{N_{Ed}}{N_{cr,v}}} \tag{3.41}$$

$$C_u = 0{,}6+0{,}4\psi_u \quad -1 \leq \psi_u = \frac{M_{2u}}{M_{1u}} \leq 1 \tag{3.42}$$

$$C_v = 0{,}6+0{,}4\psi_v \quad -1 \leq \psi_v = \frac{M_{2v}}{M_{1v}} \leq 1 \tag{3.43}$$

3.4.4 Interaction factor ξ

The ξ-factor depends on the cross-section class, Table 2.4. Its value ranges from 1 for elastic design, to 2 for plastic design, in dependence on the plate slenderness of the angle legs. More specifically it is:

- $c/t \leq 10\varepsilon$: $\quad\quad\quad \xi = 2$ $\quad\quad\quad\quad\quad\quad\quad\quad\quad\quad\quad\quad\quad$ (3.44)
- $10\varepsilon < c/t < 14\varepsilon$: $\quad \xi = \left[1 + \left(\frac{14\varepsilon-c/t}{14\varepsilon-10\varepsilon}\right) \cdot (2 - 1)\right]$ $\quad\quad\quad$ (3.45)
- $c/t > 14\varepsilon$: $\quad\quad\quad \xi = 1$ $\quad\quad\quad\quad\quad\quad\quad\quad\quad\quad\quad\quad\quad$ (3.46)

3.4.5 Justification

For angle members subjected to compression and bending, two checks for buckling around one or the other principal axis are provided. Torsional buckling is not checked separately, but is included in the local buckling check. The procedure exhibits similarities, but also differences to EN 1993-1-1, 6.3.3 (4).

Similarities:

- There are two equations for buckling around one or the other principal axis.
- The equations have three terms, one for compression, two for bending around the principal axes.
- Interaction factors $k_{i,j}$ are provided.
- LTB is included in the strong axis bending term

- Local buckling is included through the properties of the effective section

Differences

- The interaction between the three terms is not linear. The quadratic term tries to cover the cross-section resistance check as derived in et al in [3].
- Simple expressions, but straightforward from the stability theory, for the terms C_i and $k_{i,j}$ are proposed following the industry argument that *simple Codes sell steel.*

4   Experimental validation

4.1   Centric compression tests at Tsinghua University [5]

At Tsinghua University 66 tests were carried out on axially loaded pin-ended columns from equal angle sections and reported in [5]. The cross-sections ranged from L125.8 to L200.14, The material was high strength steel (HSS) S 420. Fig. 4.1 illustrates the test set-up.
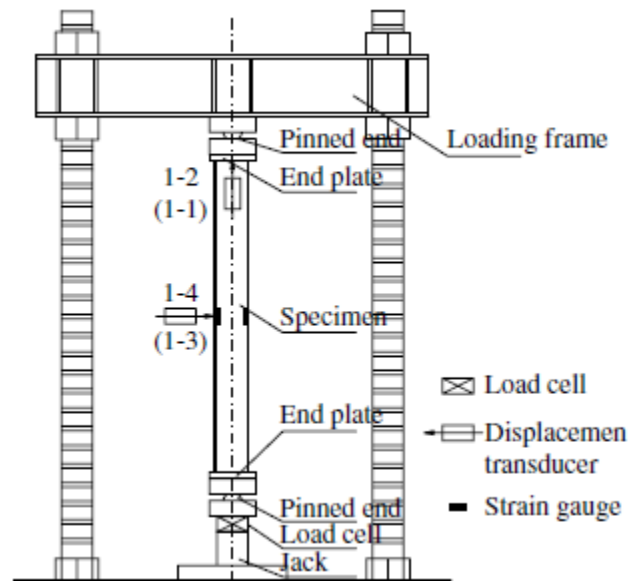
Figure 4.1: Test set-up for Tsinghua tests [5]

Fig. 4.2 presents the ratio between experimental and analytical load of the current proposal for all tests in dependence on the weak axis slenderness λ_v. The analytical load was determined using the actual geometrical and material properties without safety factors. Fig. 4.3 presents the mean value of the ratio between experimental load and analytical load according to the predictions of EN 1993-1-1 and the current proposal, while Fig. 4.4 the mean minus one standard deviation value. It may be seen that the current proposal gives a better prediction for the column capacity compared to the Eurocode 3 predictions and is always on the safe side.
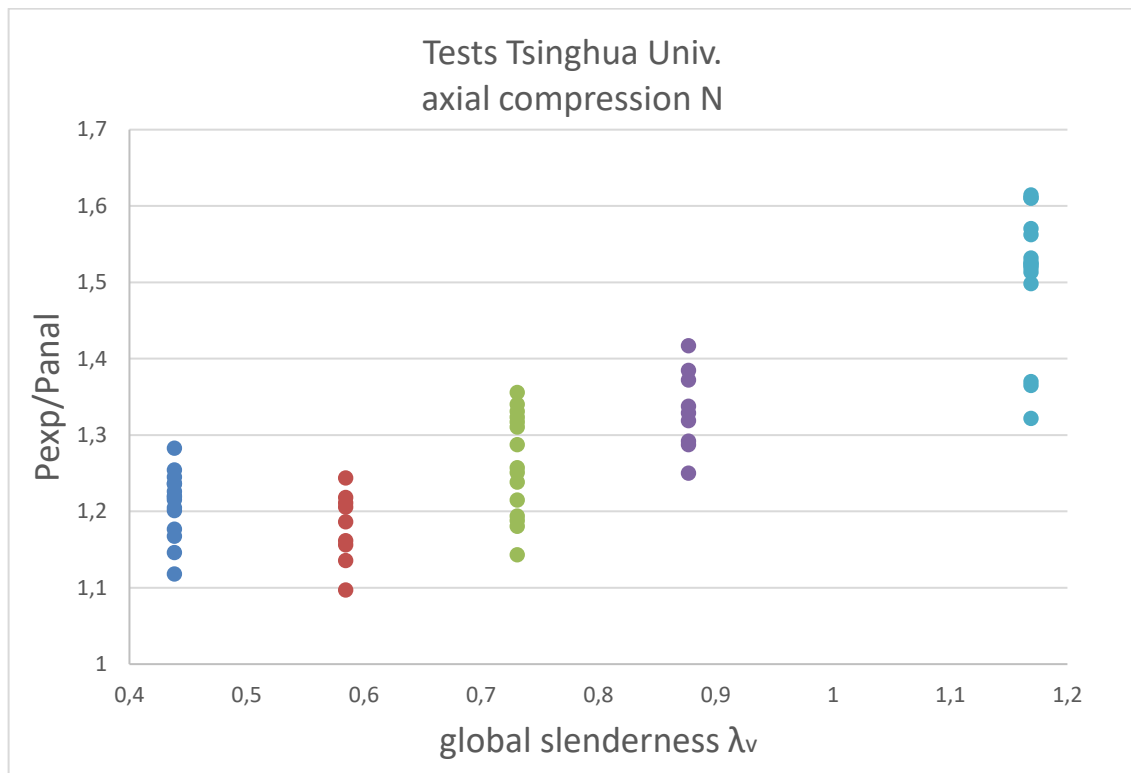
Figure 4.2: Ratio between experimental and analytical load for the Tsinghua tests
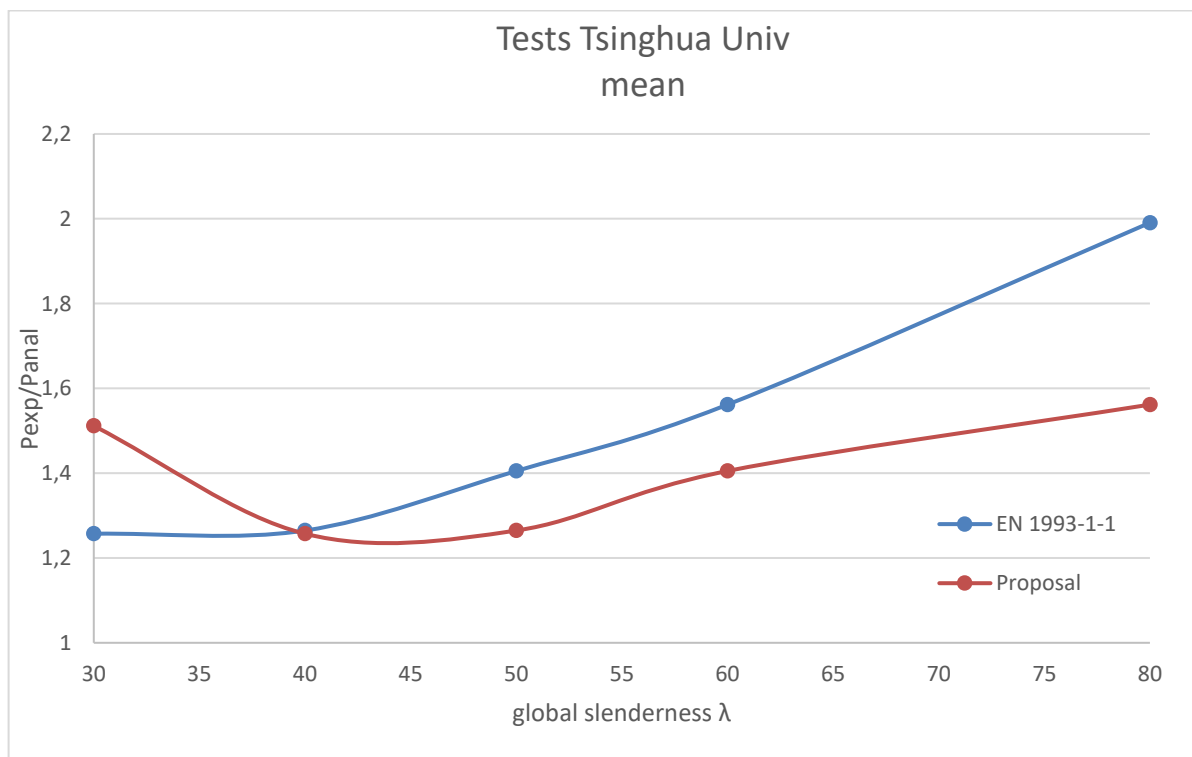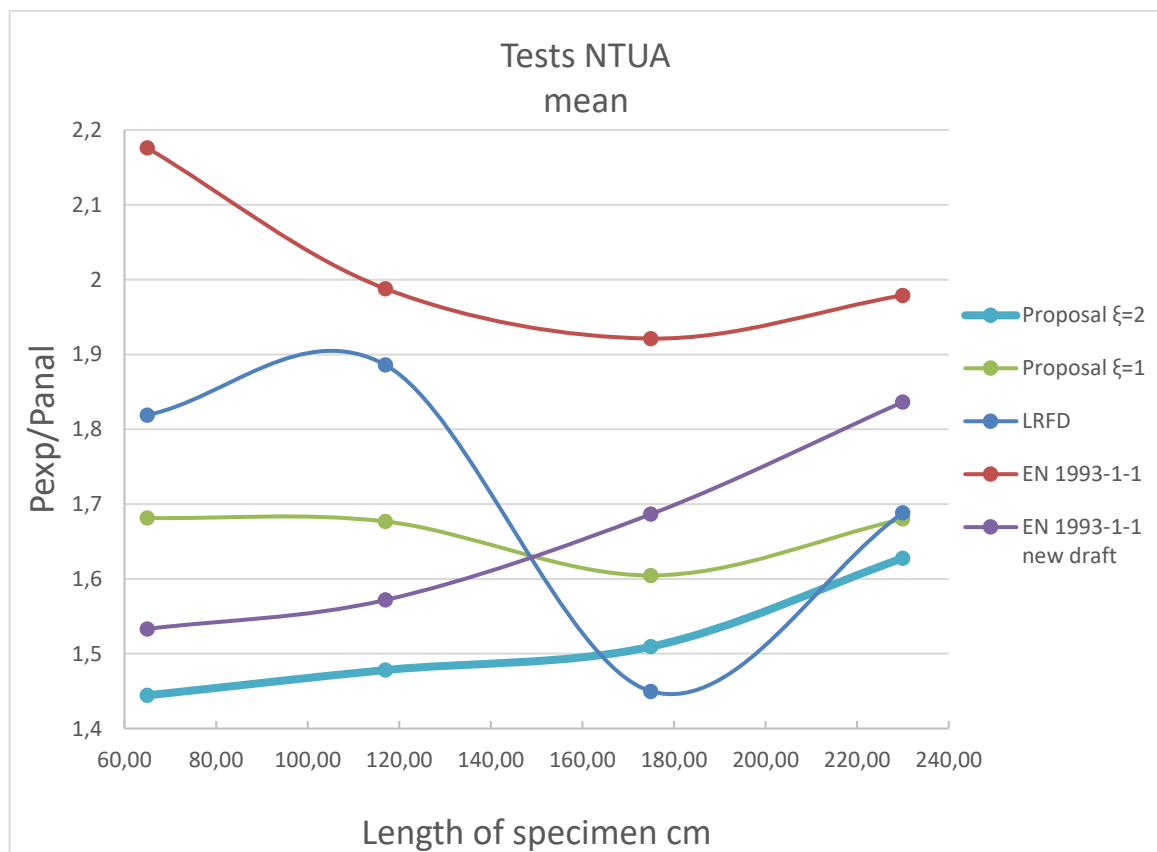

Figure 4.3: Ratio between experimental and predicted load for the Tsinghua tests, mean values
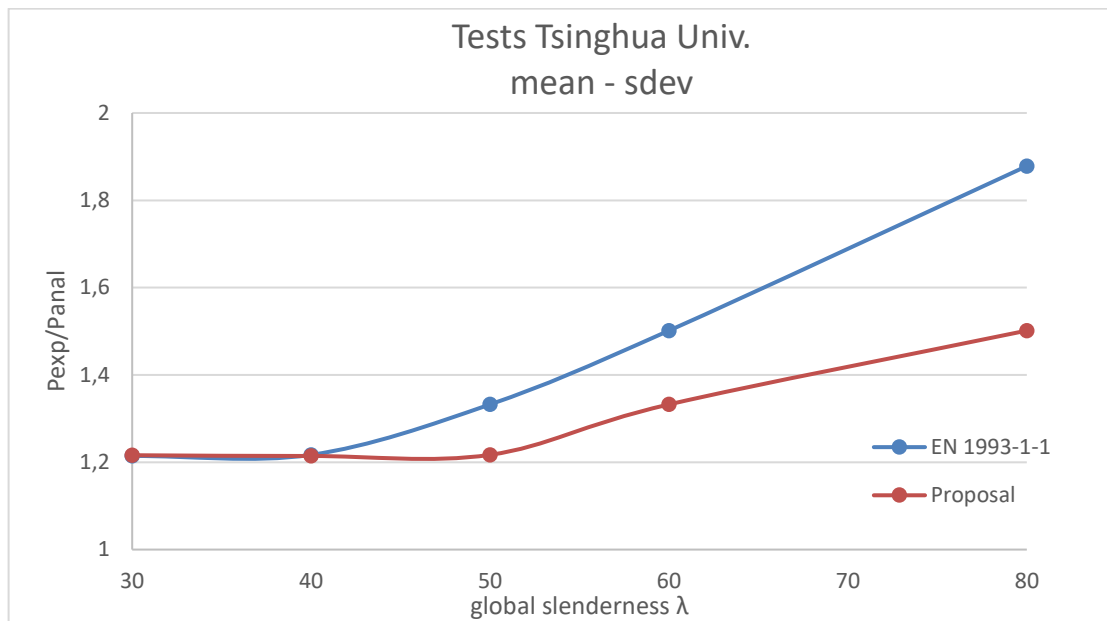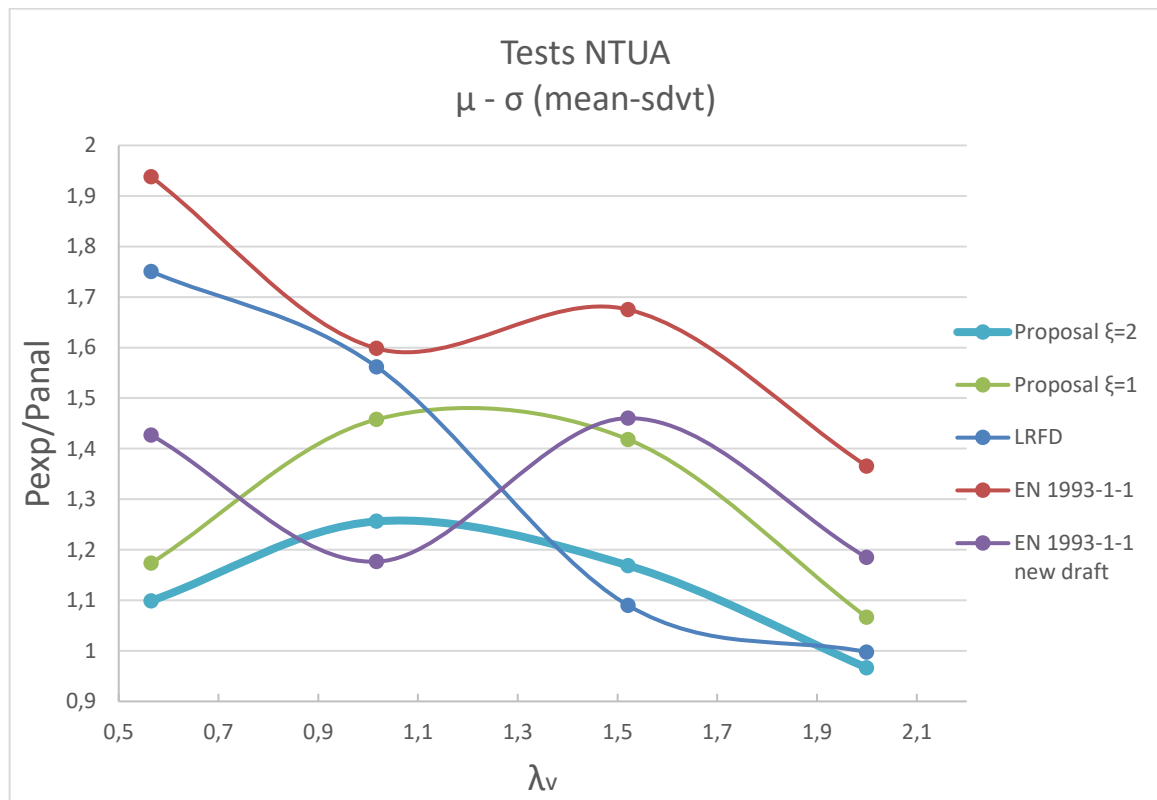
Figure 4.4: Ratio between experimental and predicted load for the Tsinghua tests, mean values minus one standard deviation

4.2 Eccentric compression tests at NTUA [7]

At the National Technical University of Athens 33 tests were carried out on axially loaded pin-ended columns with or without eccentricity and reported in [7]. The cross-sections were equal angle profiles L 70.7, the material S 275. The load was introduced through ball supports that correspond to fully hinged boundary conditions allowing free rotation in- and out-of-plane, Fig. 4.5.
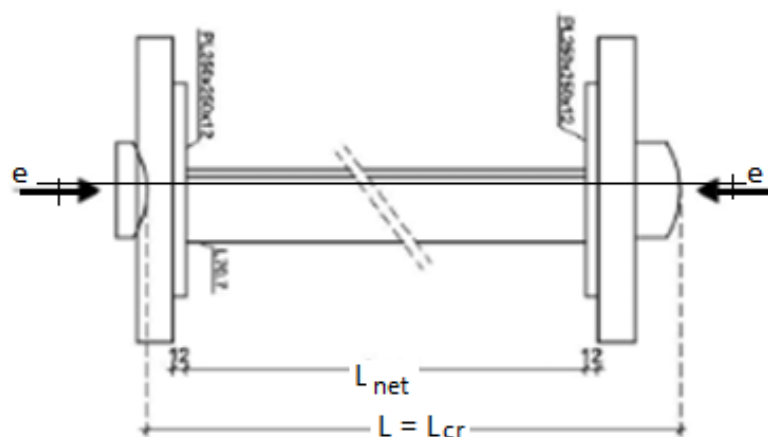
Figure 4.5: Test set-up for NTUA tests [7]

The experimental results are compared with analytic predictions from various Codes and the current proposal. More specifically, the analytical formulae considered were the following.

- The resistance formulae of the current proposal as outlined in section 3.5 with $\xi = 2$.

- The resistance formulae of the current proposal, however linearized setting $\xi = 1$.

- The resistance formulae for members to EN 1993-1-1 [2] applicable to doubly symmetric sections, equations (6.61), (6.62) with factors from method B.

- The resistance formulae for members to the new draft of EN 1993-1-1, equations (6.72), (6.73), applicable to doubly symmetric sections

- The resistance formulae of LRFD [1], applicable to angle profiles as following

  $$\frac{N_{Ed}}{2 \cdot N_{b,Rd}} + \left(\frac{M_{u,Ed}}{M_{b,Rd}} + \frac{M_{v,Ed}}{M_{v,Rd}} \right) \leq 1 \text{ or}$$

  $$\frac{N_{Ed}}{N_{b,Rd}} + \frac{8}{9} \cdot \left(\frac{M_{u,Ed}}{M_{b,Rd}} + \frac{M_{v,Ed}}{M_{v,Rd}} \right) \leq 1$$

Fig. 4.6 presents the mean value of the ratio between experimental load and analytical load as determined by the above methods, while Fig. 4.7 the mean minus one standard deviation value. Abscissa in Fig. 4.6 is the specimen's length, while in Fig. 4.7 the relative slenderness in respect to the weak axis. The analytical load was determined using the actual geometrical and material properties without safety factors. The Figures indicate that the current proposal gives a better prediction for the column capacity compared to all considered Code provisions and is always on the safe side. However, it should be said that the considered Eurocode 3 provisions apply to doubly symmetric open and closed profiles and not to angle cross-sections.

Figure 4.6: Ratio between experimental and predicted load for the NTUA tests, mean values

Figure 4.7: Ratio between experimental and predicted load for the NTUA tests, mean values minus one standard deviation

4.3   ANGELHY eccentric compression tests at ULg

At the University of Liege 10 tests were carried out on axially loaded pin-ended columns with or without eccentricity in the frame of ANGELHY. The cross-sections ranged from L150.19 to L200.21. The material was high strength steel (HSS) S 460. The load was introduced through ball supports that correspond to fully hinged boundary conditions allowing free rotation in- and out-of-plane.

The ratio between the experimental load to the axial yield load, N_{pl}, of the tests without eccentricity, together with the reduction factor χ of the European buckling curve b are illustrated in Fig. 4.8. N_{pl}, was determined using actual material properties without safety factors. It may be seen that the experimental capacities achieved are close, but a little lower than those predicted by buckling curve b. This is in contrast to the results of the Tsinghua tests [5] were buckling curve b appeared a safe prediction.

Fig. 4.9 illustrates the ratio between experimental load and analytical load determined by the current proposal as a function of the relative weak axis slenderness. The analytical load was determined using the actual geometrical and material properties without safety factors. It may be seen that the analytic method provides safe predictions for all but one test subjected to compression and bending, while for the compression tests and one compression and bending tests the prediction using the European buckling curve b overestimates the experimental capacity.
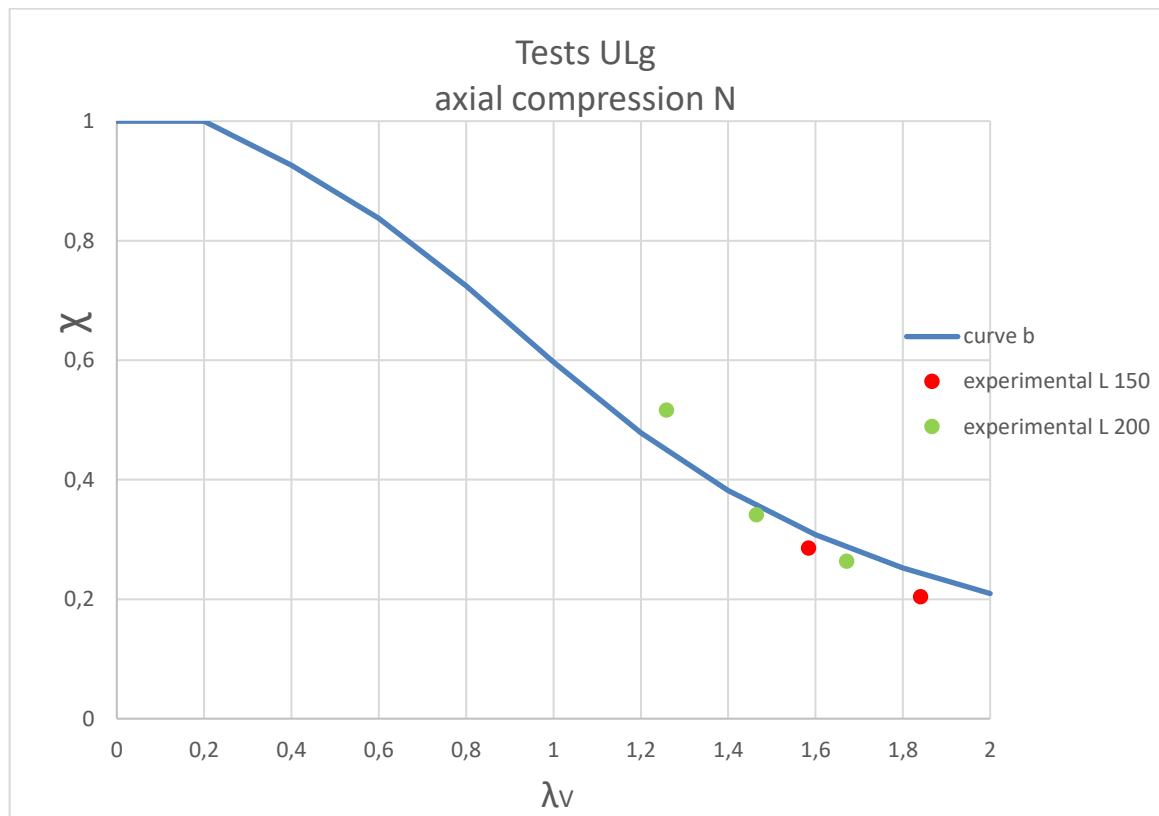
Figure 4.8: Reduction factor χ= P$_{exp}$/N$_{pl}$ for the ULg axial compression tests and the European buckling curve b
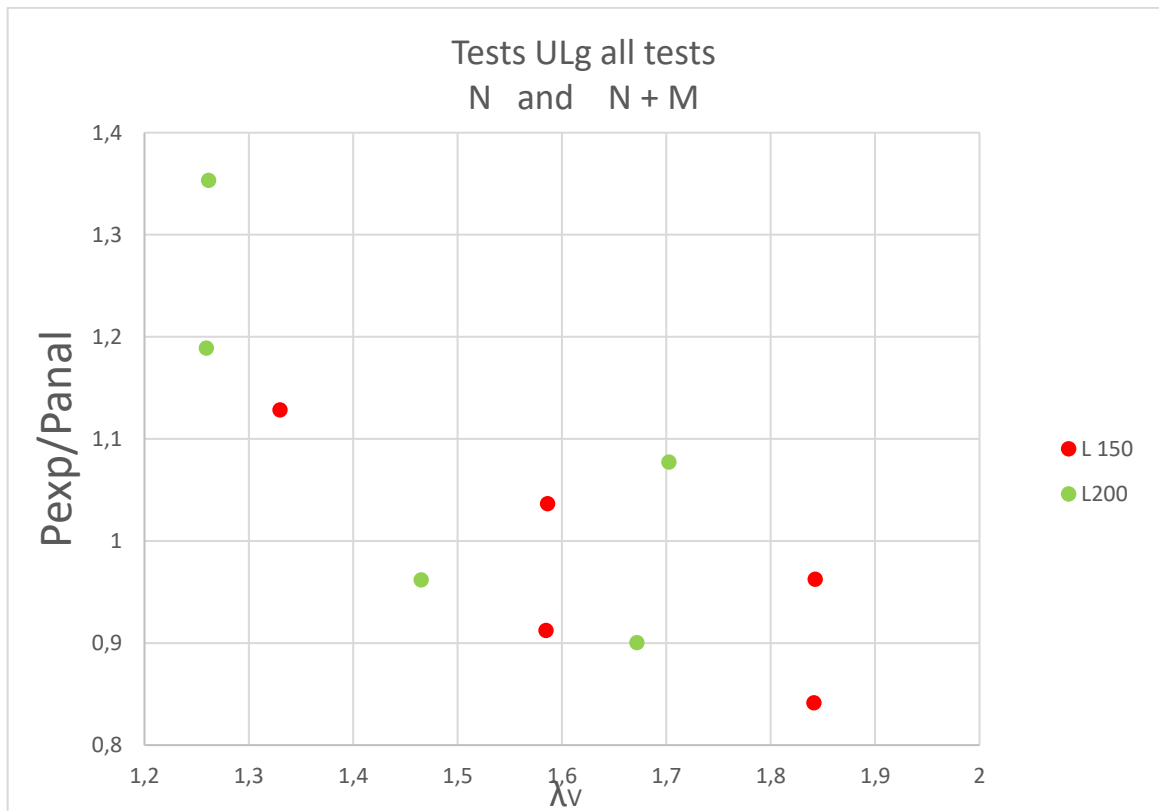
Figure 4.9: Ratio between experimental and predicted load for all ULg tests

4.4 Eccentric compression tests at TUGraz [9]

At the Technical University of Graz 27 compression tests were carried out and reported in [9] on equal angle sections, 24 on L 80.8 and 3 on L 120.12 profiles. The boundary conditions varied from clamped support (series BC1), to knife support allowing rotation in the loading plane (series BC2) and fully hinged, ball, support allowing free rotation in- and out-of-plane (series BC3), Fig. 4.10. The load was transferred through the end connections with one or two bolts. The material was S 275.
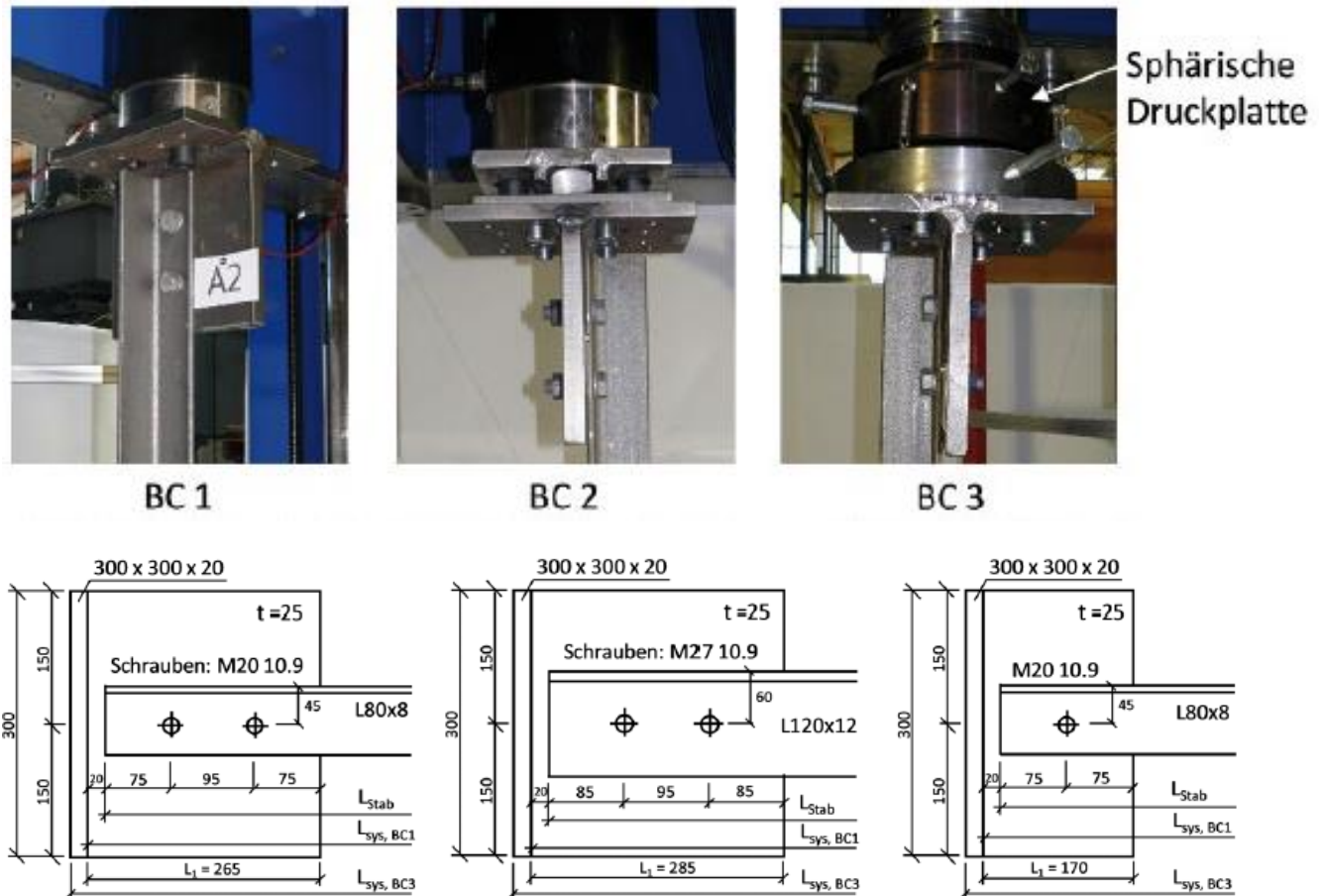
Figure 4.10: Load introduction and end support conditions of the TUGraz tests as reported in [9]

The member capacities were calculated by two methods.

1) The proposed method, checking the angle profile to compression and biaxial bending with following observations:

   a. The buckling length was set equal to the system length, L, for all cases but one. For support conditions BC1 (clamped) and connection by two bolts the buckling length was set equal to L/2.

   b. The load was introduced to the profile through one leg by the bolts. The relevant eccentricities are determined as following, Fig. 4.11.

$$e_v = \frac{e}{\sqrt{2}} - u_G$$

$$e_u = e/\sqrt{2}$$

where:

u_G is the distance of the angle's heel from its centroid along the strong axis

e is the distance of the angle's heel from the load introduction point along the leg.

The resulting moments are:

$M_u = N \cdot e_u$

$M_v = N \cdot e_v$

where N is the applied load.

The load introduction point is the center of the hole for connection with one bolt, or the center between the two holes for connection with two bolts.
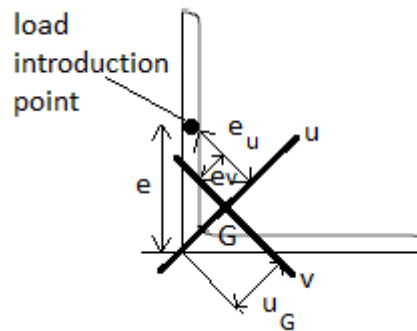
Figure 4.11: Eccentricities due to load introduction in one leg

2)   The EN 1993-3-1 method [3], in which the member is checked to compression with modified, effective, slenderness. Buckling is checked in respect to the weak, v, and the geometric, y, axes. The relevant effective slenderness is determined from:

$$\bar{\lambda}_{\text{eff,v}} = 0{,}35 + 0{,}7 \cdot \bar{\lambda}_v$$

$$\bar{\lambda}_{\text{eff,y}} = 0{,}40 + 0{,}7 \cdot \bar{\lambda}_y$$

The design resistance is determined from:

For connection with one bolt: $N_{b,Rd} = \dfrac{0{,}8\chi A f_y}{\gamma_{M1}}$

For connection with two bolts: $N_{b,Rd} = \dfrac{\chi A f_y}{\gamma_{M1}}$

where $\chi = \min\{\chi_v, \chi_y\}$

The buckling resistance is the lowest between the resistances in respect to the v- and y-axes.

Figures 4.12 and 4.13 illustrate the ratio between the experimental load and analytical load for connection with two and correspondingly one bolt, as well as the mean minus one standard deviation value for all tests. The analytical load was determined using the actual geometrical and material properties without safety factors. It may be seen that the proposed method provides safe predictions for all tests with two bolts, and all but 3 tests with one bolt. In contrast, the EN 1993-3-1 method largely overestimates the angle capacities and is on the unsafe side. The conclusion of the authors in [9] is therefore confirmed that require, in absence of appropriate design formulae, design through 2nd order system analysis accounting for member imperfections.
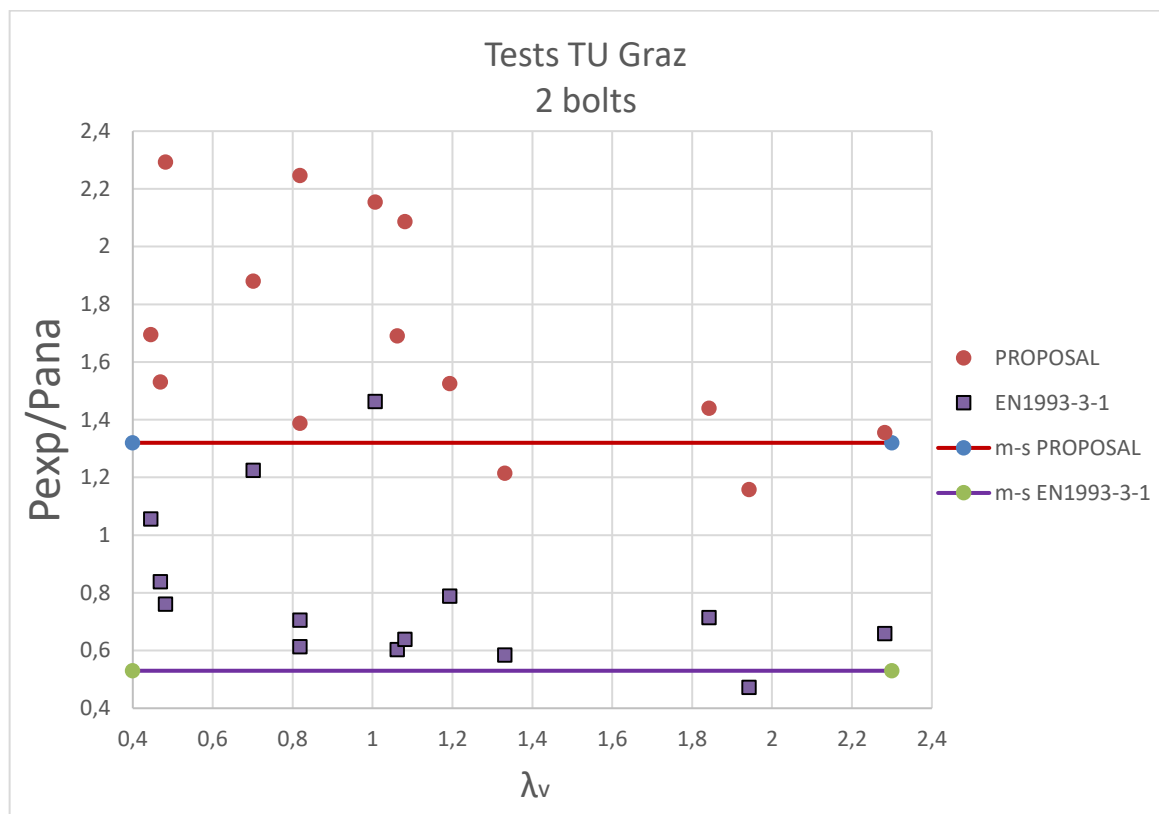
Figure 4.12: Ratio between experimental and predicted load the TUGraz tests with two bolts
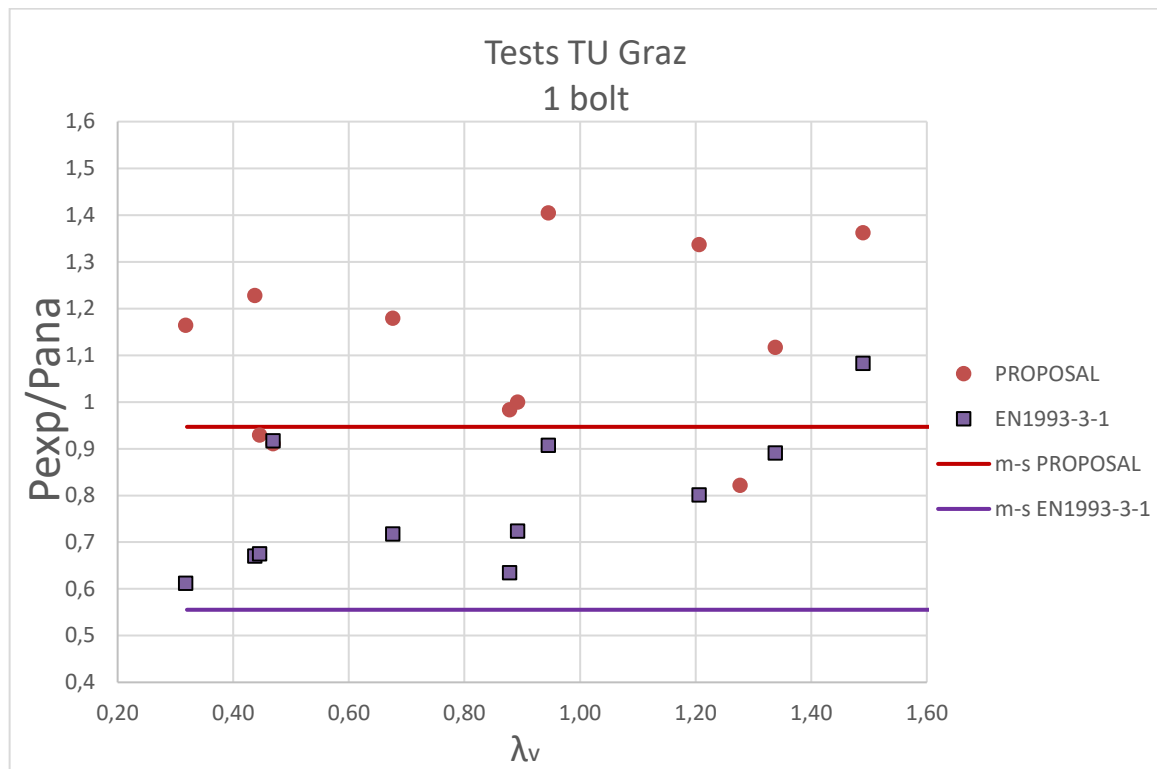
Figure 4.13: Ratio between experimental and predicted load the TUGraz tests with one bolt

4.5   Eccentric compression tests at TUBraunschweig [4]

At the Technical University of Braunschweig 40 compression tests were carried out and reported in [4] on equal angle sections L 50.5 profiles. The specimen lengths were 300, 600, 900, 1200 and 1500 mm, the material was S 355. The end support conditions were defined as clamped and hinged, Fig. 4.14. The load was introduced through one bolt M12.

Clamped bearing   Jointed bearing
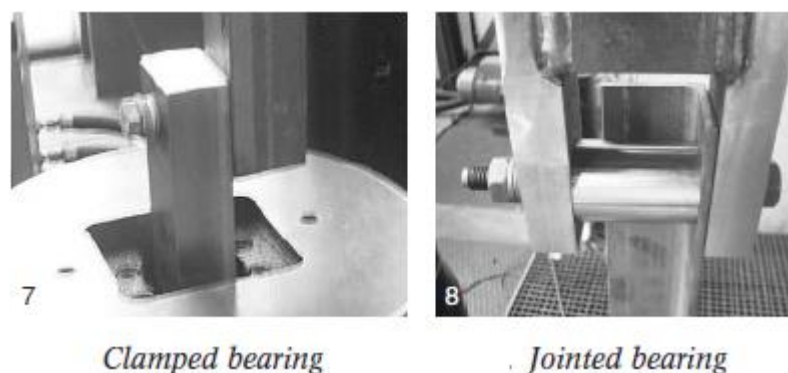
Figure 4.14: Load introduction and end support conditions of the TUBraunschweig tests as reported in [4]

Figure 4.15 presents the ratio between the ultimate load, as determined experimentally and analytically, to the axial capacity of the cross-section. In addition, the reduction factor according European buckling curve b reduced to 80% due to the connection with one bolt is presented. The analytical load was determined using the actual geometrical and material properties without safety factors. The load eccentricity was calculated as in the previous section 4.4, the buckling length was

considered equal to the system length. The Figure shows that the proposed method predicts well the experimental results, while European curve b overestimates the buckling capacity even if a 20% reduction is considered.
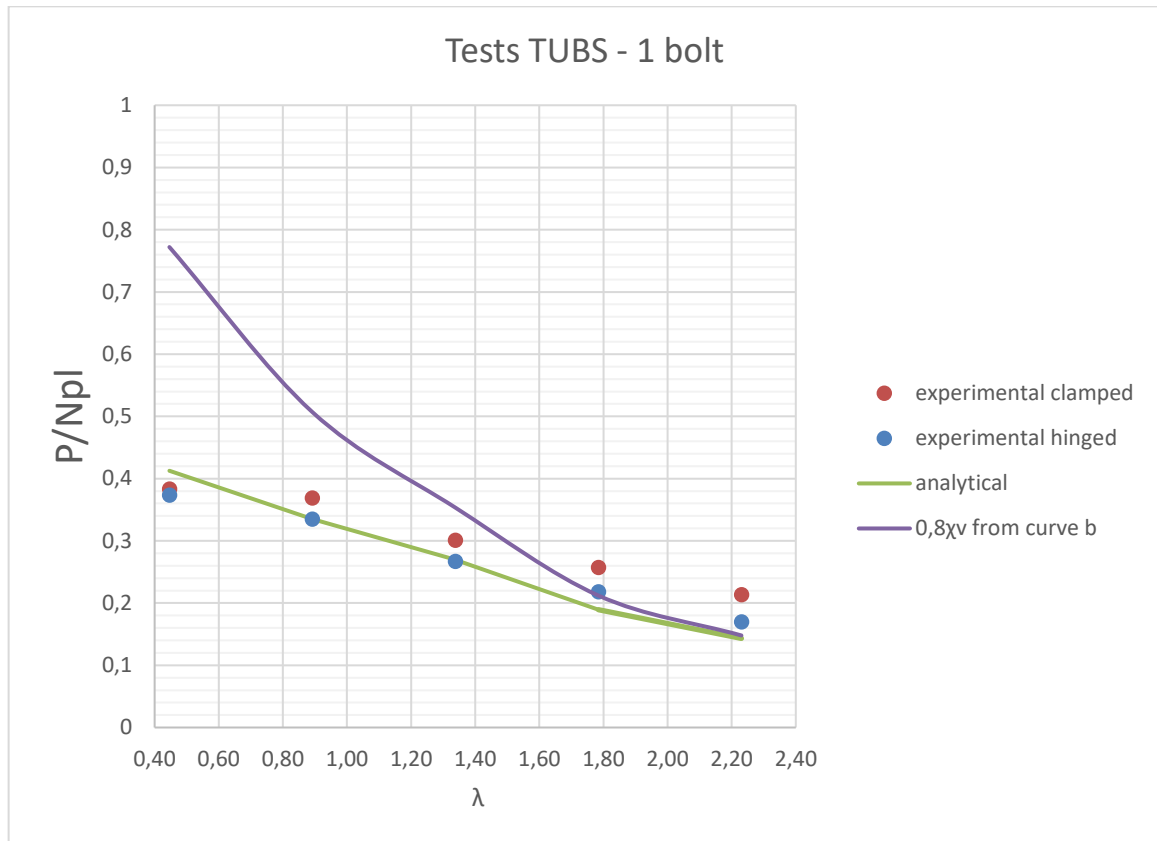
Figure 4.15: Ratio of ultimate load to plastic cross-section load

Figure 4.16 presents the ratio of the experimental to analytical load as a function of the relative weak axis slenderness. The analytical load was determined according to the proposed method and the provisions of EN 1993-3-1. It may be seen that the proposed method give best results for the hinged support conditions. The results for the clamped support seem to underestimate the buckling capacity at larger slenderness. In contrast, the provisions of EN 1993-3-1 appear to overestimate the capacity, especially for hinged support conditions. The conclusion of the authors in [4] is therefore confirmed that: "….the simplified method of EC 1993-3-1 for the one screw joint in the existing form is not wise to be used in practice".
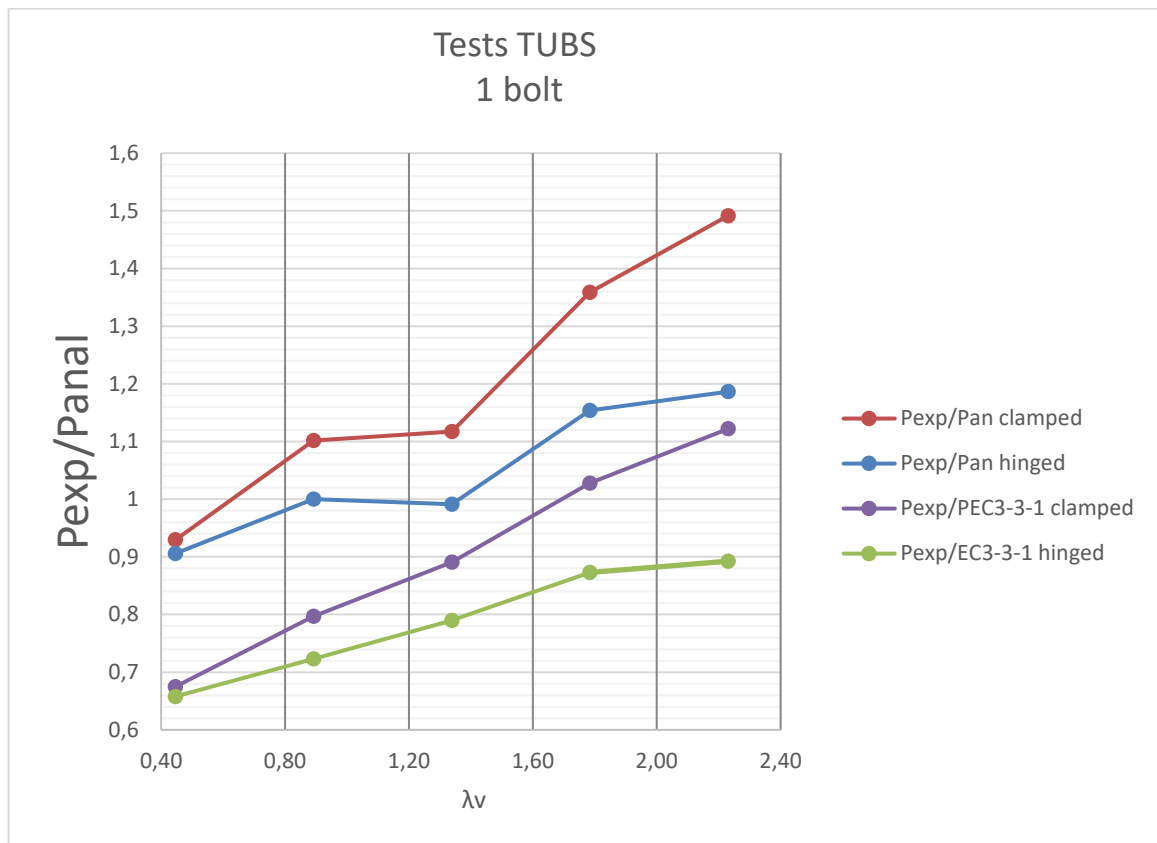
Figure 4.16: Ratio of experimental to analytical load as determined by the proposed method and the provisions of EN 1993-3-1

5 Conclusions

This report presented a design method for buckling of members composed of equal angle sections. The proposed rules are generic for the referred cross-sections and do not apply only for lattice towers. The member is subjected to combined forces and moments. The design method was validated by numerical analyses and experimental tests. Experimental results were considered from tests carried out both during the current research project, as well as during previous experimental investigations. Experimental were also compared to existing Code provisions. It was shown that the proposed method predicts well the member capacity and may be used as an alternative to existing Code provisions.

References

[1]   AISC (2000). Load and resistance factor specification for single-angle members. Am Inst Steel Construct, Chicago, IL

[2]   EN 1993-1-1 (2004). Eurocode 3: Design of steel structures – Part 1-1: General rules and rules for buildings.

[3]   EN 1993-3-1 (2006). Eurocode 3: Design of steel structures – Part 3-1: Towers, masts and chimneys –Towers and masts

[4]   Reininghaus M, Skottke M (2005) Dimensioning of pressed angle steel with one screw joint based on the standards DIN 18800 vol2 and EC1993-3-1 (towers and masts) Stahlbau 74 H7, 534-538: 40 tests

[5]   Ban HY, Shi G, Shi YJ, Wand YQ (2013). Column buckling tests of 420 MPa high strength steel single equal angles, Int. J. of Structural Stability and Dynamics, Vol. 13, No2

[6]   Vayas I, Charalambakis A, Koumousis V (2009) Inelastic resistance of angle sections subjected to biaxial bending and normal force, *Steel Construction Design and Research* 2

[7]   Spiliopoulos A, Dasiou ME, Thanopoulos P, Vayas I (2018): Experimental tests on members made from rolled angle sections, *Steel Construction Design and Research*, Volume 11, Issue 1, pp. 84-93

[8]   EN 1993-1-5 (2006). Eurocode 3: Design of steel structures - Part 1-5: Plated structural elements. CEN

[9]   Kettler M, Unterweger (2019), H. Laboratory tests on bolted steel angles in compression with varying end support conditions, Stahlbau 88 H5, 447-459

.

List of Figures

List of Tables